

**A COMPREHENSIVE BATTERY EQUIVALENT CIRCUIT BASED MODEL FOR BATTERY
MANAGEMENT APPLICATION**

Shijie Tong

Department of Mechanical and Aerospace
Engineering
University of California, Davis
Davis, CA 95616
tong@ucdavis.edu

Matthew P. Klein

Department of Mechanical and Aerospace
Engineering
University of California, Davis
Davis, CA 95616
matthewpklein@gmail.com

Jae Wan Park

Department of Mechanical and Aerospace
Engineering
University of California, Davis
Davis, CA 95616
matthewpklein@gmail.com

ABSTRACT

This paper presents a control oriented comprehensive battery model. The paper starts by presenting a battery model based on an equivalent circuit which captures particular battery characteristics of control interest. Then, the model categorizes battery dynamics based on their different response time constants (transient, long-term, life-time). Based on that, the state variables were simulated at different time steps for computational efficiency. The model used a 2-D map representing the temperature and state-of-charge dependent model parameters. Also, the model uses new battery state-of-charge and state-of-health definitions that are more practical for a real battery management system. Battery testing and simulation on various types of batteries and use scenarios was completed to validate that the model is easy to parameterize, computationally efficient and of adequate accuracy.

NOMENCLATURE

<i>ECM</i>	Equivalent circuit model
<i>BMS</i>	Battery management system
Q_{BATT}	Battery capacity
Q_{NOM}	Battery nominal capacity
<i>SoC</i>	State of charge
<i>SoC_V</i>	Voltage based state of charge
<i>SoC_C</i>	Composite state of charge
<i>SoH</i>	State of health
<i>OCV</i>	Open circuit voltage
<i>U</i>	Terminal voltage
$U_{MAX/MIN}$	Battery high and low voltage cut-off
<i>I</i>	Input current
<i>T</i>	Temperature
<i>V</i>	Voltage in battery in ECM components
<i>R</i>	Equivalent resistance in battery ECM components
<i>C</i>	Equivalent capacity in battery ECM components
I_{SD}	Self-discharge current in battery ECM
<i>AHT</i>	Battery current throughput

INTRODUCTION

Lithium ion battery systems are being considered as a promising energy storage solution because of their advantages in energy and power density, cycle durability and low self-discharge rate. Advanced battery systems have been widely used in portable electronics. The improvement in performance and decrease in price per unit makes batteries generally feasible for large scale stationary energy storage application, such as smart grids, solar and wind energy. In addition, battery systems are an important candidate for plug-in hybrid electric vehicle (PHEV) and electric vehicle (EV) energy storage. In many battery applications, in order to make informed control decisions, the battery management system is required to predict

the battery response based on measurable input and output. To serve this purpose, an ‘application-based’ battery model must 1) capture the pertinent battery characteristics as accurate as necessary, 2) have practically identifiable model parameters, 3) practical integration with the chosen battery control algorithm and be, 4) computationally efficient.

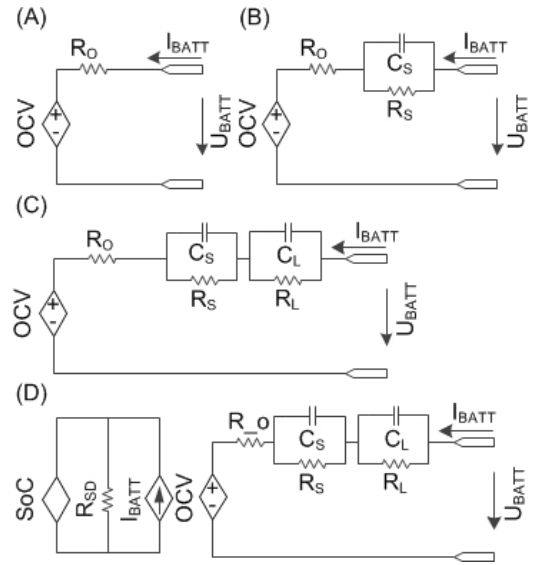


FIGURE 1. SCHEMES OF VARIOUS BATTERY EQUIVALENT CIRCUIT MODELS: (A) SINGLE RESISTOR MODEL, (B) PNGV MODEL, (C) TWO RC CIRCUIT MODEL, (D) RUN TIME BASED MODEL

The ECM is a popular solution to ‘application-based’ battery modeling. It simulates a system using networks of electrical components such as voltage sources, capacitors, and resistors [1-7]. ECM based battery models are widely used because they are able to simulate a battery system’s electrical performance; they are also physically justifiable with limited insights of battery cell electrochemical reactions in a lumped sense. A simple battery ECM is a voltage source in serial with a resistor as shown in Figure 1(A) [8]. This type of model is easy to parameterize, integrate into performance simulations [9, 10] and be used for state estimation [11]. For some applications, the prediction results of the single-resistor ECM is too responsive and unable to capture the charge transfer phenomenon that occurs in a battery. A step further is to add a paralleled RC circuit to the single-resistor model shown in Figure 1(B) [12]. This type of ECM can be parameterized using a hybrid pulse power characterization (HPPC) test schedule (Figure 7). [3, 13]. For some modern battery chemistries, such as LiFePO4 positive electrode, the transient response of a battery possesses both short and long time-constants. An ECM with two RC branches and one serial resistor as shown in Figure 1(C) provides a satisfactory fit to the battery transient response [14-16]. A battery ‘Run Time’ based ECM model presented by Min et al. [7, 17], as shown in Figure 1(D), adds a ‘Run Time’ section that includes self-discharge and capacity fading into the model.

A comprehensive battery model representing battery performance over the entire battery life may include the following characteristic functions: 1) available capacity as a function of cycle number, temperature, and current; 2) available capacity as a function of storage time; 3) OCV as a function of state-of-charge (SoC); and 4) transient response to electrical loads. Many model structures have been proposed by others that partially incorporate the above characteristics, but a complete model covering all of the above characteristics while maintaining the specific capability of being integrated into a BMS has not yet been developed. Also, for a model to be integrated into the battery management application it should require only simple parameterization tests and be computationally efficient to keep hardware costs at a minimum. Consequently, this paper follows the steps of modeling, parameter identification and simulation to validate the advantages of the proposed model. Section 1 presents the battery ECM modeling with detailed model components. Section 2 introduces the model parameter identification platform and simulation of the model in state space form. Section 3 describes battery tests conducted. Section 4 covers results and discussion of the testing, model parameters identification and simulation. Conclusions are drawn in section 5.

1. BATTERY EQUIVALENT CIRCUIT MODELING

The scheme of the proposed comprehensive battery ECM is illustrated in Fig. 2. The model includes three sub-models to cover the dynamics of the different response times: transient model, long-term model and life-time model. The battery transient model represents the dynamic response to instantaneous current and temperature loads. When batteries are under use, the transient model predicts battery open-circuit-voltage (OCV) and efficiency. The long-term model represents SoC variation due to cycling and self-discharging. The life-time model captures battery degradation of total capacity over cycling and calendar aging. Fundamental model variables were defined as follows

Definition: A battery's *high voltage cut-off* and *low voltage cut-off* is a pair of voltage limits specified based on battery chemistries that should not be exceeded during operation.

Definition: A battery is *fully charged* after constant 1C charging until the voltage reaches the high cut-off and remains constant until the current has dropped to C/20.

Definition: A battery is *fully discharged* after the low voltage cut-off is reached during a 1C discharge.

Definition: A battery's *total capacity* C_{BATT} is the total charge removed from the battery fully charged state to fully discharged state via 1C. This paper will use Ah as the unit of capacity.

Definition: A battery's *nominal capacity* C_{NOM} is the total capacity of a fresh cell. In this paper the C_{NOM} value specified by the battery manufacturers were used.

Definition: A battery's *SoH* is the total capacity divided by the nominal capacity.

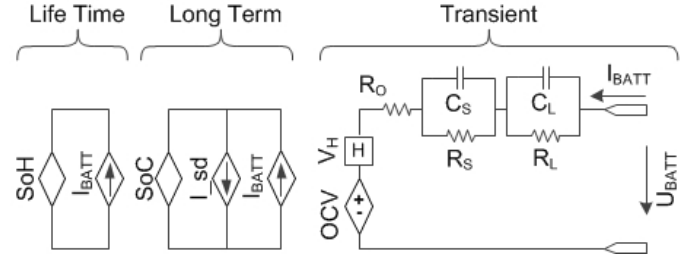


FIGURE 2. PROPOSED BATTERY COMPREHENSIVE ECM MODEL

Transient model

The transient model represents the battery terminal voltage U_{BATT} as the sum of five voltage components

$$U_{BATT} = V_L + V_S + V_O + V_H + OCV \quad (1)$$

V_L and V_S are transient response voltages of long and short time constants (voltages across R_S and R_L), V_O is the ohmic voltage loss (voltage across R_O), and V_H is the hysteresis voltage.

V_L and V_S are solved by integrating the current through the RC branch circuit

$$\frac{dU_S}{dt} = \frac{-1}{R_S C_S} U_S + \frac{1}{C_S} I_{BATT} \quad (2)$$

$$\frac{dU_L}{dt} = \frac{-1}{R_L C_L} U_L + \frac{1}{C_L} I_{BATT} \quad (3)$$

and

$$V_O = R_O I_{BATT} \quad (4)$$

V_H adds a zero state hysteresis term to the model

$$V_H = P_1 s(I_{BATT}) I_{BATT} \quad (5)$$

where

$$s(i) = \begin{cases} 1, & i > 0.1 \\ -1, & i < -0.1 \\ s(i), & -0.1 < i < 0.1 \end{cases}$$

P_1 is half of the difference between two voltage measurements after charge or discharge and 1 hour rest as indicated in Fig. 3.

OCV values can then be evaluated by taking the mean of two voltage measurements (solid line in Fig. 3).

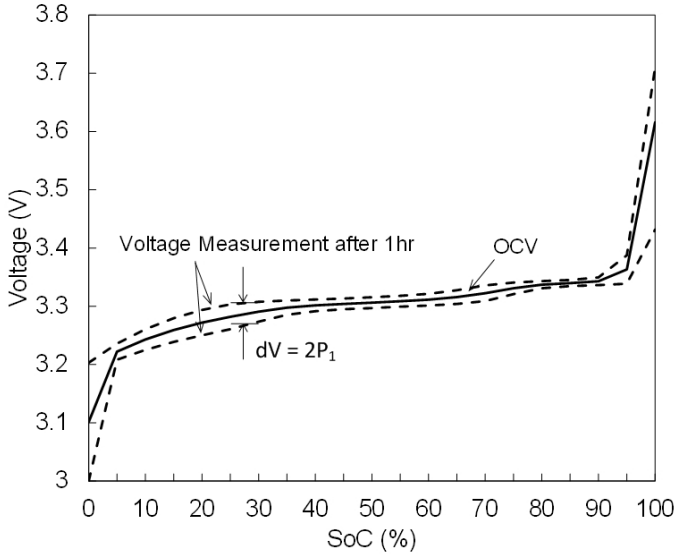


FIGURE 3. OPEN CIRCUIT VOLTAGE AND HYSTERESIS VOLTAGE ESTIMATED VIA VOLTAGE MEASUREMENT AFTER 1HR RESTING

Long-Term Model

Battery SoC is indicated by coulombic counting and by referencing the battery OCV. However, in high power-energy ratio applications, battery operation limits were usually enforced by voltage cut-offs rather than an SoC limitation. As illustrated in Figure 4, given the battery high and low voltage cutoffs to be 2.8V and 4V, when the battery is charged or discharged at 1C it is cycled through the full range from 0% SoC to 100% SoC as shown by the dashed line in Fig. 4. However, when cycled at 2C, dotted line in Fig. 4, it cannot reach 100% of the range due to the voltage cutoffs. In this paper, the SoC function was defined as follows

Definition: A battery's *state-of-charge* SoC is estimated by current integration

$$\frac{dSoC}{dt} = \frac{1}{C_{BATT}} (I_{BATT} + I_{SD}) \quad (6)$$

where I_{SD} is the estimated self-discharge current. SoC can also be estimated through $OCV(SoC)$ function look up.

Definition: A battery's *voltage based state-of-charge* SoC_V indicates the battery state of charge by simply monitoring the battery terminal voltage. Referring to the example in Figure 3, when $U_{BATT} = 2.8$, $SoC_V = 0\%$; $U_{BATT} = 4.0$, $SoC_V = 100\%$.

$$SoC_V = (U_{BATT} - U_{MIN}) / (U_{MAX} - U_{MIN}) \quad (7)$$

Definition: A battery's *composite state-of-charge* SoC_C is a weighted combination of SoC_V and SoC

$$SoC_C = (1 - w)SoC + wSoC_V \quad (8)$$

w is a weighting factor that makes SoC the only indicator for SoC_C when U_{BATT} is not close to the voltage cutoffs and makes SoC_V the primary SoC_C indicator when approaching voltage cut-offs

$$w = \begin{cases} 0, & 10\% < SoC_V < 90\% \\ (1 - 2SoC_V)^2, & SoC_V < 10\% \text{ or } SoC_V > 90\% \end{cases}$$

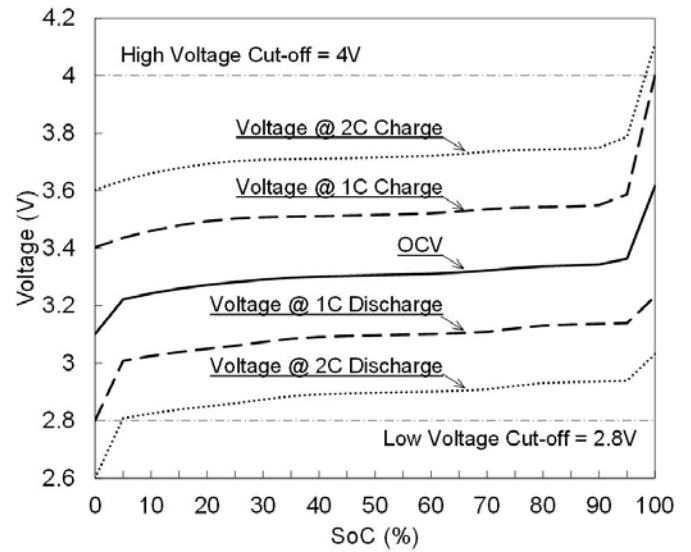


FIGURE 4. OPEN CIRCUIT VOLTAGE, TERMINAL VOLTAGE AT 1C CHARGE AND DISCHARGE, TERMINAL VOLTAGE AT 2C CHARGE AND DISCHARGE

Life-Time Model

The life-time model summarizes the battery degradation pattern based on an observed change in the SoH and battery use history. The model takes the function as follows

$$SoH = 1 - (P_2 AHT_{BATT} + P_3 AHT_{SD})^{1/2} \quad (9)$$

P_2 and P_3 are curve fitting parameters. AHT is the battery current throughput and t is the storage time. The life-time model is unlikely to provide a reliable prediction of battery aging process based operation history of a single or small number of batteries. However, in many battery applications such as an

electric vehicle or stationary energy storage, very large quantities of batteries are used. The life-time model identified based on a large number of batteries usage history will be a valuable reference for battery management. Even though the long-term model is only shown here to analyze the capacity degradation it can be easily extended to analyze internal resistance degradation as well by monitoring the change in the model resistance parameters.

2. MODEL IMPLEMENTATION

SoC and temperature dependent parameter mapping

Parameters in the proposed model are SoC and temperature dependent. A 2-D map was adopted to cast varying parameters onto their dependent states and to be referred to by the model. The empirically constructed 2-D map covers parameter values over the full operation range of the battery.

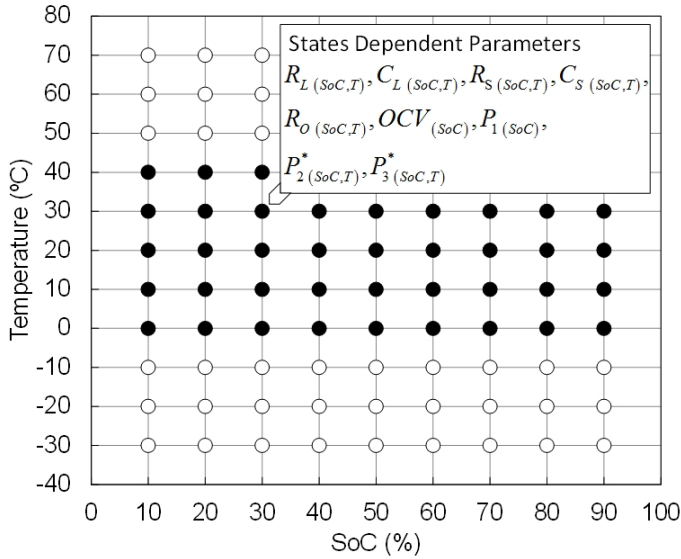


FIGURE 5. MODEL STATES DEPENDENT PARAMETERS ARE MAPPED ON A 2-D MAP (FILLED DOTS INDICATING KNOWN PARAMETERS VALUES, HOLLOW DOTS INDICATING UNKNOWN PARAMETERS VALUES)

As illustrated in Fig. 5, a battery system with proper thermal and electrical management operates within temperatures ranging from 0 to 40 °C and SoCs ranging from 10% to 90%, and only within these states the model has known parameter values. Note that the battery degradation process is highly related to cell temperature and SoC. As a result, the curve fitting parameter P_2 and P_3 (marked with star in Fig. 5) are SoC and temperature dependent. However, a large amount of empirical data is required to draw an accurate estimation of parameter P_2 and P_3 . As a result, the battery management's scope is to use pre-identified P_2 and P_3 . The tradeoff here is that having a large lookup table is far more computationally efficient than needing to solve a large set of physically based partial-differential equations in real-time. Some evaluation methods of P_2 ~ P_4 will

be presented based on battery testing in the Results and Discussion section.

Model implementation

The model should be simulated by three different time steps. The transient model takes the smallest time step Δt_1 . The long-term model takes bigger time step $\Delta t_2 = m\Delta t_1$. The life-time model takes the largest time step $\Delta t_3 = n\Delta t_2 = nm\Delta t_1$. When the model is applied to the BMS to identify model parameters the same set of time steps apply. The model is rewritten in discretized state space form below

$$\begin{aligned} X_{N+1} &= A_N X_N + B_N u_N \\ Y_N &= C_N X_N + D_N u_N \end{aligned} \quad (8)$$

where

$$\begin{aligned} X &= \begin{pmatrix} SoC \\ V_L \\ V_S \\ (1-SoH)^2 \end{pmatrix}, Y = U_{BATT}, u = \begin{pmatrix} I_{BATT} \\ I_{SD} \end{pmatrix} \\ A &= \begin{pmatrix} 1 & 0 & 0 & 0 \\ 0 & \exp(-\Delta t_1 / R_L C_L) & 0 & 0 \\ 0 & 0 & \exp(-\Delta t_1 / R_S C_S) & 0 \\ 0 & 0 & 0 & 1 \end{pmatrix} \\ B &= \begin{pmatrix} \Delta t_1 / C_{BATT} & \Delta t_2 / C_{BATT} \\ R_L (1 - \exp(-\Delta t_1 / R_L C_L)) & 0 \\ R_S (1 - \exp(-\Delta t_1 / R_S C_S)) & 0 \\ \Delta t_3 P_2 \text{sign}(I_{BATT}) & \Delta t_3 P_3 \end{pmatrix} \\ C &= [P_4 \quad 1 \quad 1 \quad 0] \\ D &= [R_O + P_5] \end{aligned}$$

the constant $P_5 = OCV/SoC$ to be looked up from function $OCV(SoC)$.

3. BATTERY TESTING

Battery tests are performed to demonstrate that the proposed ECM can be identified use battery input/ output measurement and to validate the battery model in a real application. To show that the battery works for various chemistries four types of batteries were selected as test samples as listed in Tab. 1.

TABLE 1. BATTERY CELLS USED FOR TESTING

	Material (Cathode- Anode)	C_{NOM} (Ah)	Voltage cut-offs (V)	Type
CELL1	LiFePO-C	14	2~3.65	Pouch
CELL2	LiNiCoMn-C	10	2.8~4.2	Pouch
CELL3	LiFePO-C	1.1	2~3.65	Cylindrical

Battery testing was performed using an Arbin Instruments BT2000 battery testing station with a TestEquity temperature chamber as shown in Fig. 6.



FIGURE 6. BATTERY CYCLER AND TEMPERATURE CHAMBER

Steady capacity and HPPC testing

Proposed by the PNGV battery testing manual, steady capacity tests and HPPC tests provide the necessary data to quantify the battery capacity and estimate dynamic characteristics. First, the battery is fully charged; Second, the battery is fully discharged. Third, after a full charge the battery is discharged by 10% of its capacity followed by a 1 hour rest. Following this a 10 second discharge pulse, 10 second rest and 10 second charge pulse are performed and again 10% SoC is discharged followed by a 1 hour rest. An example test schedule is plotted in Fig. 7.

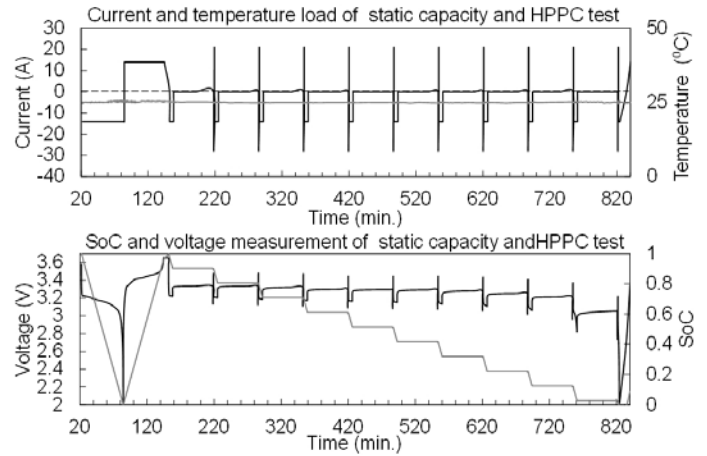


FIGURE 7. STEADY CAPACITY AND HPPC TESTING SCHEDULE

To identify the model parameters that are temperature dependent multiple HPPC tests are performed on single cells with different constant environmental temperature settings.

Vehicle drive cycle testing

The vehicle drive cycle test simulates an automotive environment. The test profile was generated using the MATLAB-based ADVISOR vehicle simulator software representing a battery cell's usage in a Chevy Volt plug-in hybrid vehicle. As illustrated in Figure 8, the battery is exposed to varying temperatures ranging from 0°C to 40 °C, and is repetitively cycled with UDDS, HWY, and US06 vehicle driving profiles.

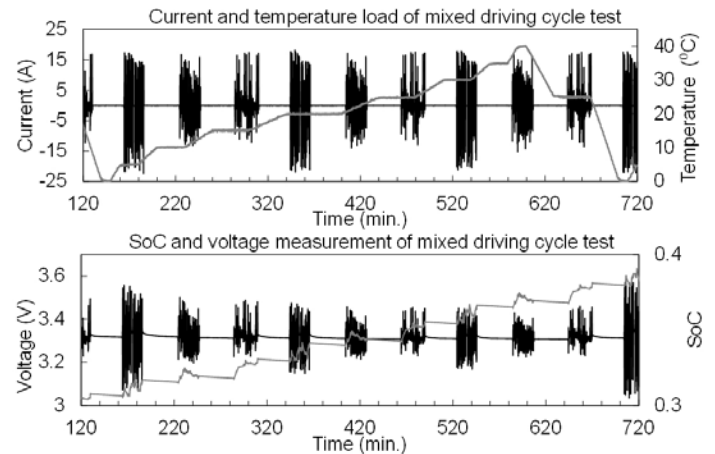


FIGURE 8. DRIVE CYCLE TESTING SCHEDULE

Accelerated cycle and calendar aging testing

Batteries lose capacity as cycle life and calendar life degradation increases. Tests were conducted to achieve accelerated aging of cells. The cycling aging test was performed by cycling a cell at -15 °C. Meanwhile the battery was cycled

using a US06 driving profile. Calendar aging tests were performed by storing 5 cells in a temperature chamber set to constant 70 °C with SoC levels varying from 25% to 100%.

Battery tests conducted on different cells are summarized in Tab. 2.

TABLE 2. BATTERY CELLS AND THEIR TESTING SCHEDULE

Quantity	Test	Note	
CELL1	1	SC+HPPC	Tested at temperature of 10 °C, 20 °C, 30 °C, 50 °C
CELL2	1	SC+HPPC	Tested at temperature of 15 °C, 25 °C, 35 °C, 45 °C
CELL1	1	Drive Cycle	
CELL3	5	Cycle Aging	Each of 5 cells is cycled with 0,50,100,150,200 cycles
CELL3	5	Calendar Aging	Each of 5 cells is stored with initial SoC of 100%,90%,75%,50%,25 %

4. RESULTS AND DISCUSSION

Model parameters identification

Figure 9 presents the model parameter identification results of CELL1. This is a LiFePO-Graphite based cell. The battery input and output data was extracted from Steady Capacity and HPPC test results. As indicated in Fig. 9(A)(C)(E), the battery equivalent resistance R_O , R_L , and R_S increases as the battery SoC decreases and the temperature is decreased. Also, battery model transient response time constant ($C_L R_L$) peaks when the SoC approaches 0% and 100%. As a result, the battery has longer charge transfer process at low and high SoC. As shown in Fig. 9(F), the OCV(SoC) has a flat curve from 10% SoC to 90% SoC, but varies rapidly when approaching 0% and 100%.

Figure 10 presents the model parameter identification results of CELL2. This is a LiNiCoMn-Graphite based cell. As indicated in Fig. 10(A)(C)(E), the battery equivalent resistance R_O , R_L , and R_S follows the same trend with respect to temperature and SoC as CELL1. Different from CELL1, CELL2's time constant of long transient response is much longer as shown in Fig. 10(C)(D) that the voltage contribution of V_L can be ignored. The internal resistance is higher than CELL1 resulting in lower efficiency. As shown in Fig. 10(F), the OCV(SoC) function of CELL2 varies more than CELL1 but in a linear format .

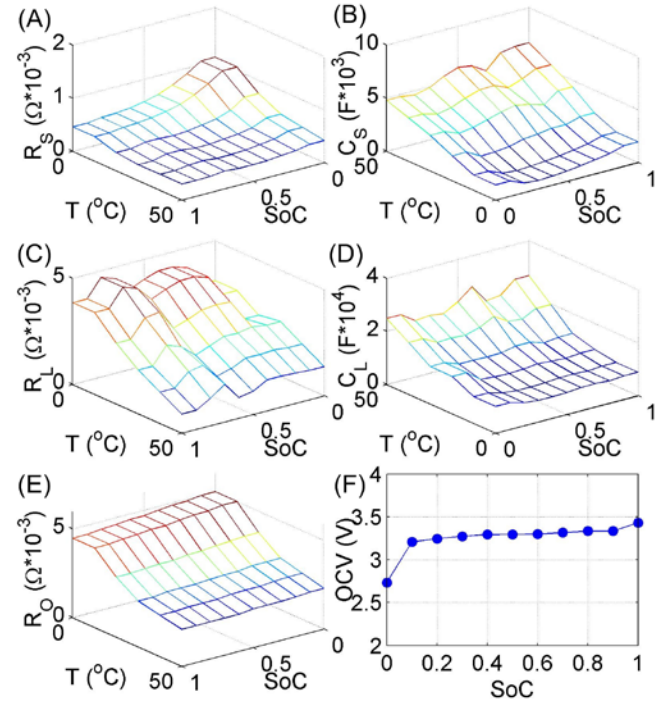


FIGURE 9.IDENTIFIED TRANSIENT MODEL PARAMETERS OF CELL1

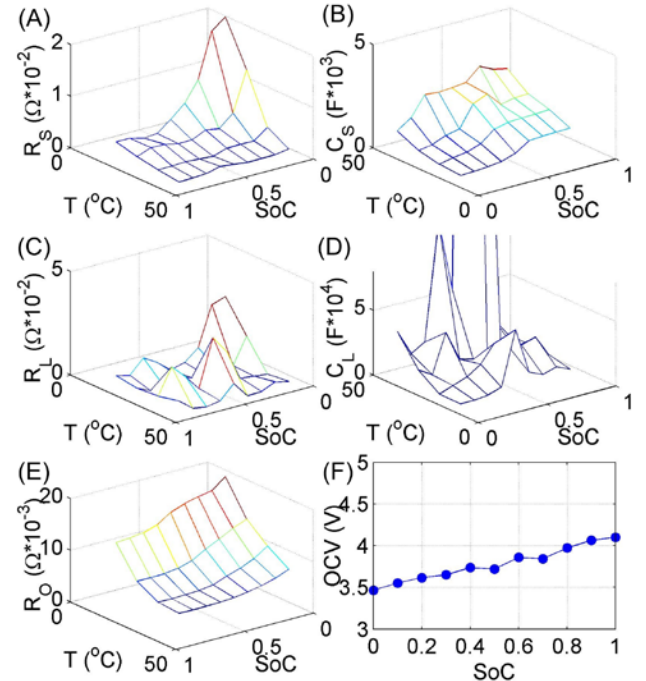


FIGURE 10.IDENTIFIED TRANSIENT MODEL PARAMETERS OF CELL2

These two sets of test results indicate that batteries of difference chemistries can be well presented by the proposed model. The model parameters can be identified by simply using the battery input and output measurements.

Battery aging test results are shown, in Tab.3

TABLE 3. BATTERY CELLS AND THEIR TESTING SCHEDULE

Cell #	Test Condition	SoH Before Test	SoH After Test
1	50 cycle @-15 °C	100%	89.3%
2	100 cycle @-15 °C	100%	78.9%
3	200 cycle @-15 °C	100%	79.7%
4	100% SoC Storage @ 70 °C	100%	62.8%
5	90% SoC Storage @ 70 °C	100%	65.2%
6	50% SoC Storage @ 70 °C	100%	76.9%
7	25% SoC Storage @ 70 °C	100%	86.2%

Using observation results and battery operation history, battery empirical ageing model can be estimated. The summarized aging model will be helpful for battery life optimization

Simulation

Utilizing parameterized the model of CELL1 and data from the vehicle drive cycle testing conducted on CELL1, the model simulated battery voltage output under varying temperature loads (ranging from 0 to 40 degree C) and under varying current loads (a mixed drive cycle profile includes US06, HWY, UDSS drive cycle scaled down to a single cell level). A truncation of the model input is shown in the upper plot of Fig. 11, the predicted voltage output based on the proposed model and its estimation error compared to actual measurement was shown in the lower plot of Fig. 11. The average error for voltage prediction was less than 5%. The proposed model is validated to be of good accuracy under varying load conditions.

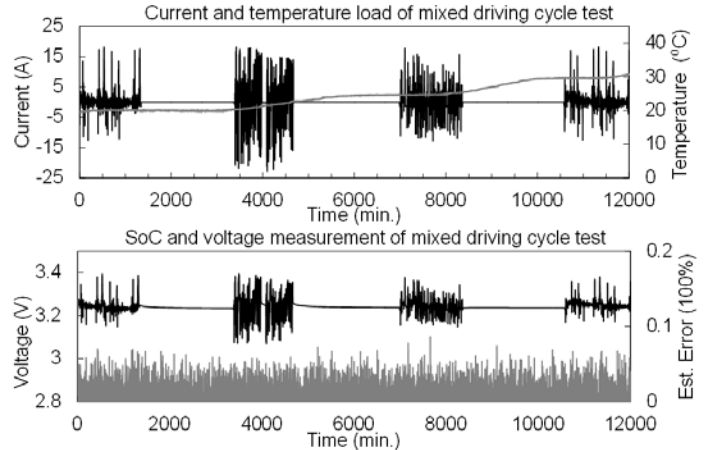


FIGURE 11. DRIVE CYCLE TEST AND SIMULATION RESULT

CONCLUSION

This paper has presented a new ECM based model directly designed to be integrated into a BMS for the purpose of SoC and SoH estimation. First, a review of some of the more common equivalent circuit models was presented, which include the simple single-resistor model, the Thevenin model, a dual RC-Thevenin model and finally the 'Real Time' model. Essentially, they grow in complexity in an effort to track a battery's dynamics more completely. For example, the simplest single-resistor model can only capture a generalized instantaneous voltage response for the cell and has no time response at all. The RC elements are then added to improve the transient accuracy, however then when one concerns a design around the full life of the battery pack that time dynamic becomes important as well. The model presented here expands further on this notion and couples three models of vastly varying time dynamics to efficiently model all pertinent dynamics of a battery throughout its entire life.

After proposing our model and discussing how it alleviates the need for a practical and simple to implement model for estimation in a real-time setting data was presented for the battery types of battery testing that could be used to parameterize this model. The simplest tests used are the capacity test and HPPC test at different constant temperature set-points. This is then executed over the entire range of temperatures that will be seen for the given application. Dynamic drive cycle testing may be used to either replace or build upon the HPPC data set and run at various temperature set-points. Finally, the ageing tests that were used covered both throughput and calendar affects and a low temperature cycle test was run in parallel to high temperature storage tests to expedite degradation.

Lastly, the model parameters were validated through simulation and comparison to the test data to quantify the accuracy it is able to provide on the three main response times it covers.

Paper Number

ASME assigns each accepted paper with a unique number. Replace **DSCC2008-12345** in the above title with the paper number supplied to you by ASME for your paper.

REFERENCES

- [1] H. Xiao, L. Shaohua, S. Stanton, and L. Wenyu, "A Foster Network Thermal Model for HEV/EV Battery Modeling," *Industry Applications, IEEE Transactions on*, vol. 47, pp. 1692-1699, 2011.
- [2] B. Yannliaw, "Modeling of lithium ion cells?A simple equivalent-circuit model approach," *Solid State Ionics*, vol. 175, pp. 835-839, 2004.
- [3] B. Y. Liaw, R. G. Jungst, G. Nagasubramanian, H. L. Case, and D. H. Doughty, "Modeling capacity fade in lithium-ion cells," *Journal of Power Sources*, vol. 140, pp. 157-161, 2005.
- [4] V. Agarwal, K. Uthaichana, R. A. DeCarlo, and L. H. Tsoukalas, "Development and Validation of a Battery Model Useful for Discharging and Charging Power Control and Lifetime Estimation," *Energy Conversion, IEEE Transactions on*, vol. 25, pp. 821-835, 2010.
- [5] Z. Jiucui, C. Song, H. Sharif, and M. Alahmad, "Modeling Discharge Behavior of Multicell Battery," *Energy Conversion, IEEE Transactions on*, vol. 25, pp. 1133-1141, 2010.
- [6] I. Papic, "Simulation model for discharging a lead-acid battery energy storage system for load leveling," *Energy Conversion, IEEE Transactions on*, vol. 21, pp. 608-615, 2006.
- [7] K. Taesic and Q. Wei, "A Hybrid Battery Model Capable of Capturing Dynamic Circuit Characteristics and Nonlinear Capacity Effects," *Energy Conversion, IEEE Transactions on*, vol. 26, pp. 1172-1180, 2011.
- [8] V. H. Johnson, "Battery performance models in ADVISOR," *Journal of Power Sources*, vol. 110, pp. 321-329, 2002.
- [9] S. X. Chen, K. J. Tseng, and S. S. Choi, "Modeling of Lithium-Ion Battery for Energy Storage System Simulation," in *Power and Energy Engineering Conference, 2009. APPEEC 2009. Asia-Pacific, 2009*, pp. 1-4.
- [10] O. Tremblay, L. A. Dessaint, and A. I. Dekkiche, "A Generic Battery Model for the Dynamic Simulation of Hybrid Electric Vehicles," in *Vehicle Power and Propulsion Conference, 2007. VPPC 2007. IEEE, 2007*, pp. 284-289.
- [11] G. L. Plett, "Extended Kalman filtering for battery management systems of LiPB-based HEV battery packs: Part 3. State and parameter estimation," *Journal of Power Sources*, vol. 134, pp. 277-292, 2004.
- [12] PNGV, "PNGV Battery Test Manual Rev. 3," 2001.
- [13] M. A. Roscher and D. U. Sauer, "Dynamic electric behavior and open-circuit-voltage modeling of LiFePO4-based lithium ion secondary batteries," *Journal of Power Sources*, vol. 196, pp. 331-336, 2011.
- [14] M. C. Knauff, C. J. Dafis, D. Niebur, H. G. Kwatny, and C. O. Nwankpa, "Simulink Model for Hybrid Power System Test-bed," in *Electric Ship Technologies Symposium, 2007. ESTS '07. IEEE, 2007*, pp. 421-427.
- [15] H. Dai, X. Wei, Z. Sun, J. Wang, and W. Gu, "Online cell SOC estimation of Li-ion battery packs using a dual time-scale Kalman filtering for EV applications," *Applied Energy*, vol. 95, pp. 227-237, 2012.
- [16] H. He, X. Zhang, R. Xiong, Y. Xu, and H. Guo, "Online model-based estimation of state-of-charge and open-circuit voltage of lithium-ion batteries in electric vehicles," *Energy*, vol. 39, pp. 310-318, 2012.
- [17] C. Min and G. A. Rincon-Mora, "Accurate electrical battery model capable of predicting runtime and I-V performance," *Energy Conversion, IEEE Transactions on*, vol. 21, pp. 504-511, 2006.